

Analysis of airborne SAR data (L-band) for discrimination land use/land cover types in the Brazilian Amazon region

João Roberto dos Santos; Fábio G. Gonçalves; Luciano V. Dutra; José C. Mura; Waldir R. Paradella

INPE – National Institute for Space Research

São José dos Campos – SP, Brasil

{jrberto, fabiogg, waldir}@dsr.inpe.br ; {dutra, mura}@dpi.inpe.br

Abstract - The objective of this paper is to show the potential of multi-polarized mosaic-images from a MAPSAR (L-band) simulation campaign performed in the Amazon region (test site Tapajós) in order to discriminate land use/land cover classes. An Enhanced-Frost filter was used and the thematic discrimination was done by an algorithm for attribute extraction based on Bhattacharya distance. A comparison was made among the radiometric aspects of the SAR mosaic for 10 thematic classes obtained, converting these B-distances to JM distance values. This allowed to define which individual or multiple polarizations are more appropriate for the identification of thematic classes.

Keyword: tropical forest, SAR-R99B, monitoring, land use, land cover, remote sensing, Amazon.

I. INTRODUCTION

The Brazilian Amazon has suffered important changes of land cover/land use due to the human activities, resulting a loss and fragmentation of habitat, which are the major threats to biological diversity. The annual monitoring of the land use dynamics of the entire Amazon forest with these optical images is restricted by the high frequency of cloud cover in certain regions of this ecosystem. A multi-temporal analysis of TM-Landsat data done (timeframe of 12 years) used to estimate the annual gross deforestation rate in the Brazilian Amazon region shows that 21%, in average, from the imaged areas were cloud covered. This has caused uncertainties of the estimated values for these annual deforestation rates. The use of imaging radars is one of the most important options to complement information and to obtain a better accuracy at this type of mapping, contributing also for the inventory and forest monitoring of the Amazon region. Observing the current international space programs, one verifies several imaging radars, such as ENVISAT/SAR, ALOS/PALSAR, RADARSAT-2, TerraSAR, whose contributions for the survey of tropical areas will be added to those done recently by other airborne and spaceborne SAR systems [1], [2], [3] and [4].

The cooperation between INPE (Brazil) and DLR (Germany) for the analysis on the viability of the construction project of an orbital SAR (MAPSAR) in L-band were developed [5]. The simulation campaign was done using the sensor SAR-

R99B from SIPAM, onboard of an EMB-145 aircraft. In this context, a SAR simulation phase was done with image acquisition over several areas, considering different themes in the Amazon: agriculture, cartography, forestry, geology, hydrology, coastal zones, defense/intelligence.

So the objective of this work is to show the potential of the MAPSAR mosaic-images, to characterize the variations of forest cover considering measurements of statistical separability among multi-classes, using as test-sites some representative landscape sections in the region of the Tapajós National Forest - FLONA (S 3° 01' 59,85" to S 3° 10' 39,33" and WGr 54° 59' 53,08" to WGr 54° 52' 44,96").

II. SAR MOSAIC CHARACTERISTICS AND METHODOLOGICAL APPROACH

In the MAPSAR configuration the following characteristics are foreseen: variation of the incidence angle by rotation of the satellite, ten beams providing images with different attributes of spatial resolution (3m, 10m and 20m) polarizations (unique, dual and quad-pol) and distinct width of swath [5]. The mosaics of images generated this way can simulate the frequency of the orbital SAR (L-band), the HH, VV and HV polarizations, the viewing geometry in descending orbit and incidence angles corresponding to the beams in far range 8 (42,22° – 45,24°), range 9 (45,16° – 46,92°) and range 10 (46,28° – 48,08°). The SAR simulation however was restricted only to the mode of average resolution under high incidence angle (far range mode), whose limitation was conditioned by the restriction of imaging with low incidence angle of SAR-R99B. Being so, a set of images derived from 10 acquisitions with lateral superposition was used, allowing the generation of L_{HH} , L_{VV} and L_{HV} polarized mosaics related to the far range mode of MAPSAR simulation. Histogram equalization functions, available at the ER-Mapper software package were used to work at the cuts of swaths of polarimetric images, in the process to obtain the mosaics.

From the polarized mosaic we defined the interpretation potential, considering four sections of study representing the investigated landscape. An Enhanced-Frost filter (windows size 5x5) was used at the radar image to remove speckle, but

preserving high frequency edges, according to [6 and 7]. Based on thematic training plots of different formats and sizes, totaling 12,200 pixels), the quantitative analysis of the class discrimination was done using an attribute extraction algorithm [8], based on the Bhattacharya distance, whose estimated value (B) represents the square of the normalized distance between the class means. This B-distance was converted in the Jeffreys-Matusita (JM) distance by equation

$$JM_{ij} = 2(1 - e^{-B})$$

Whose separation measure is a much more reliable criterion, presumably because as a function of class separation, it behaves much more like probability of correct classification [9]. Such JM-distance values were afterwards associated graphically to the probability of correct classification.

A field survey campaign was done simultaneously to the SAR mission and several observation samples of the landscape and of sites of forest inventory, all duly geo-referenced, were used to understand the potential of SAR mosaics in the thematic survey. Corner reflectors (14) were distributed within the area under study to provide information for the radiometric and geometric calibration of SAR images.

III. RESULTS AND DISCUSSIONS

Figure 1 shows a section of a SAR mosaic used in this study. This mosaic was filtered by an E-Frost filter and 45 representative samples of classes were obtained: recent deforested areas (1), bare soil (2), degraded forest (3), primary forest(4), alluvial forest(5), forest with old timber exploitation(6), old secondary succession(7), crop areas(8), clean pasture(9) and overgrown pasture (10). At Figure 2 one observes the examples of radar response of L_{HH} and L_{VV} polarizations associated with some important land cover types at Tapajós region. In this scatterplot one sees the space of attributes occupied by each class, whose diagram is formed by the variance of gray levels from sampling/class, values of the first and fourth quartile and also by the median value. In the summarized analysis of the graphic representations one verifies that the average gray levels are adequately coherent, with higher values for the typology of higher biomass value and with a better defined forest structure. This gradation of values diminishes proportionally to the occurrence of different human effects in the forest, such as the selective logging activities (with the occurrence of clearings caused by cutting of trees and by the opening of trails to transport the logs) or even the total forest conversion in pasture or agricultural area. Generally, there is a remarkable amount of overlap among the radiometric response from certain thematic classes, specially at those which still conserve more similar contents of biomass.

Based on the JM-distance dataset derived from all combinations of thematic classes mentioned above, considering the use of isolated or the combination of 2 or 3 polarizations combined, one affirm generically:

- a) Taking into account only the largest JM-distance

values among classes for just one polarization, the average JM value is 1.5305 with correct classification probability around 95%, from these samples used for training. From the 45 possible thematic combinations in this case of isolated polarization, the L_{HH} image was superior (42%) to the other two polarizations, for all class discrimination;

- b) In the case of the set of two polarizations, JM-distance reached 1.6397, with the HV polarization presenting an important participation in the binomial of polarized images. The L_{HH-HV} and L_{VV-HV} datasets represent together ~75% of the discrimination performance of the investigated classes;
- c) Once when the simultaneous integration of the three polarizations is considered, the JM value was 1.6732, indicating a correct classification probability of ~96.43%. It is important to inform that the relation between the separability measure of classes and the theoretical values of probability is nonlinear.

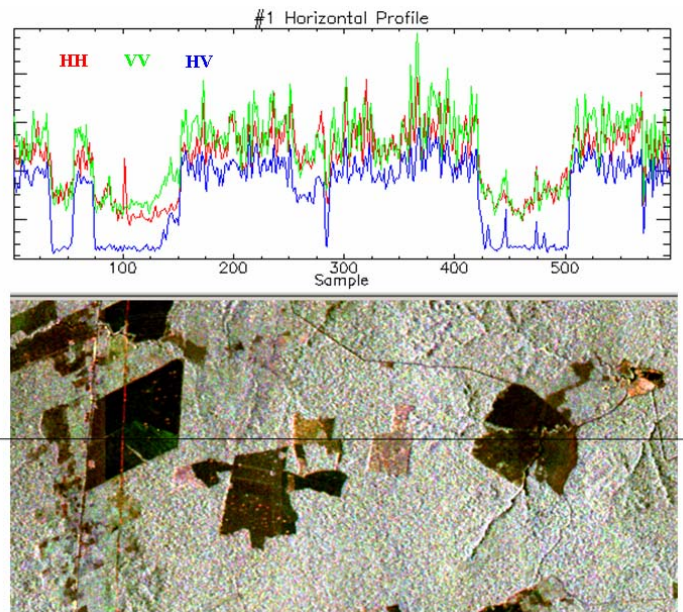


Figure 1. Behavior of different targets at the landscape in the SAR mosaic-images of multi-polarized L-band data from the Tapajós region. The L-band response of the recent deforestation can be observed at position 350 (axis x) of this profile.

The landscape of this region presents a complexity of aspects: a significant preservation area referring to FLONA (Tapajós National Forest) with remnants of ecosystems from open and dense forests; another one, also within FLONA, in a previously established stands, where there are, since long times, timber exploitation activities within the norms of sustainable management; external sections of FLONA where there is an accelerated conversion rate of other types of land use, specially for the enlargement of the agricultural frontier, with extensive soybean plantations.

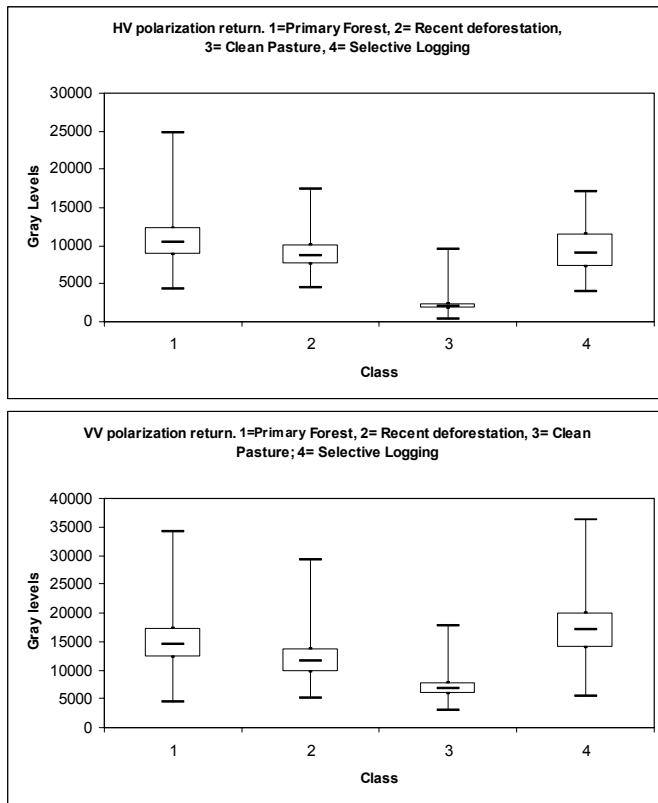


Figure 2. Examples of radiometric statistical attributes of some land cover classes at the mosaic images of L_{HV} and L_{VV} .

One of the issues of this study was to verify the discrimination capacity between “primary forest” and other land cover classes on the SAR-R99B images, considering specially the exploration activities (selective logging) or forest conversion (recent deforestation). At Table 1 one observes that the highest JM-distance values of this class (primary forest) and the other ones mentioned above, allows the following correlations:

- The average probability values of classification reaches $\sim 95\%$ when both polarizations are simultaneously used, and it was established that the pair L_{VV-HV} is the multi-polarized set with the best discrimination contribution ($\sim 55\%$) of the thematic variability;
- Comparing the class “primary forest” with those classes of intensive land use (crop, clean pasture or overgrown pasture) one verifies that the space of attributes from these L-band data are well defined, specially for the polarization VV, presenting JM-distances above 1.95;
- once the “primary forest” suffers an initial clear cut process, called “recent deforested area” (where all woody and foliar material is still in place when the SAR L-band data were acquired), the best statistical separation measure between these two classes is $JM = 0.8689$ for the isolated VV polarization with a correct classification probability around 82.6%. Such performance can be increased using the set of three polarizations with a JM-distance of 1.2342, which

represents around 89% of the accuracy probability expected in the classification, if we want to discriminate just these two thematic classes. The isolated use of L_{HH} band presents a lower value of JM-distance (0.0784), indicating the difficulty for the discrimination of the class “recent deforested areas” using only this polarization, according to [3]. It is important to record that the primary forest has an aboveground biomass of ~ 220 ton/ha, and the volumetric and double bounce scattering mechanism are distributed through several forest strata.

- In the case of discrimination capacity between areas of primary forest and those with timber exploitation activities, the best JM value (0.4423) was derived from the set of three polarizations. This value equals to a low performance in the separation of these two classes, because in the area of Tapajós FLONA the timber exploitation has been done by sustainable management, i.e. with low degradation impact. Furthermore, those areas imaged and sampled with SAR from this typology are not areas of recent exploitation, which allows to state that a recovery process in the intermediate forest strata is under development. The timber exploitation regime established there is considered as a withdrawal of $25m^3/ha$ of wood in average.

Table 1. JM-distance values among “primary forest” and other land cover classes, considering the applicability of E-Frost filter on the L-band MAPSAR simulation scene.

Class Pair	One polarization	Two Polarizations	Three polarizations
4-1	0.8689 (VV)	1.1191(VV- HH)	1.2342
4-2	1.9875 (HV)	1.9918(VV -HV)	1.9926
4-3	1.9023 (HH)	1.9276(HH- HV)	1.9442
4-5	1.6272 (HH)	1.9004(HH- HV)	1.9080
4-6	0.3625 (VV)	0.4109(VV- HH)	0.4423
4-7	0.8689 (VV)	1.0264(VV- HV)	1.1102
4-8	1.9828 (VV)	1.9932(VV- HH)	1.9939
4-9	1.9994 (VV)	1.9999(VV- HV)	1.9999
4-10	1.9911 (VV)	1.9977(VV- HV)	1.9982

(1) Recently deforested areas; (2) Bare soil; (3) Degraded forest; (4) Primary forest; (5) Alluvial forest; (6) Forest with old timber exploitation; (7) Old secondary succession; (8) Crop areas; (9) Clean pasture; (10) Overgrown pasture.

Additional analysis are being done that allow the description of polarimetric characteristics of forest targets from a new series of attributes which include: the phase difference ($\Delta\phi$), and the polarimetric coherence (γ) among polarizations HH and VV; the entropy (H), the anisotropy (A) resulting from the decomposition by auto-vectors from the coherence matrix [10]; and the components of volumetric scattering (P_v), double-bounce (P_d) and superficial bounce (P_s), resulting from the incoherent decomposition of the co-variance matrix [11]. All these efforts allow the identification of scattering

mechanisms of natural media employing differences in the polarization signature (Figure 3) for purposes of forest classification and also for the estimation of biophysical parameters.

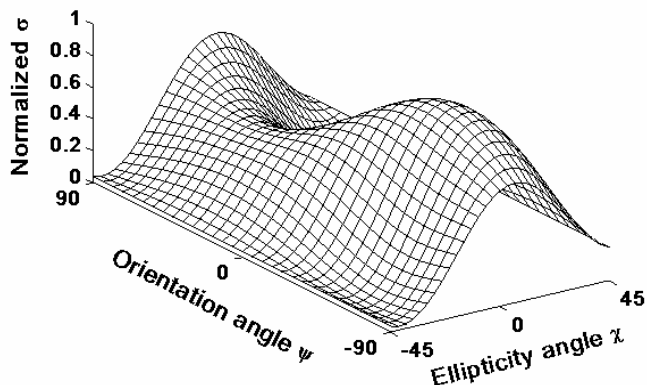


Figure 3. Polarimetric L-band response of forest under timber exploitation. This response indicates that the highest values of σ occur at linear polarizations ($\chi = 0^\circ$), with preferentially horizontal orientation ($\psi = \pm 90^\circ$). Possibly this dependence is the result of a structure with a more homogeneous canopy and most twigs of trees that compose the upper stratum are oriented horizontally.

IV. CONCLUSIONS

The results indicate the capacity of mosaic-images from SAR-R99, in its multi-polarized mode, to discriminate between several land use/land cover classes, proving that this experiment is very significant for the simulation of MAPSAR. The procedure for data analysis, using statistical separation measurements among multi-classes, was adequate to show the individual performance or the set of the different polarizations available from SAR R99B system (L- band). This experiment and its performance should also be the basis for studies with dual-polarized ALOS/PALSAR data, whose program strategy is a systematic acquisition of images over the Amazon region, contributing to studies on inventory and forest monitoring.

Acknowledgements

Special thanks go to CNPq (research grants), LBA and PETROBRAS. Thanks are extended to CENSIPAM (Manaus) for the airborne SAR-99B data and to DLR/German for helpful support for the MAPSAR simulation.

REFERENCES

- [1] S. Saatchi; B. Nelson; E. Podest; J. Holt. Mapping land cover types in the Amazon basin using 1Km JERS-1 mosaic. *International Journal of Remote Sensing*, vol. 21, n. 6, pp. 1201-1234, 2000.
- [2] J.R. Santos.; M.S.W. Pardi Lacruz; L.S. Araujo; M. Keil. Savanna and tropical rainforest biomass estimation and spatialization using JERS-1 data. *International Journal of Remote Sensing*, vol. 23, n.7, pp. 1217-1229, 2002.
- [3] R. Almeida Filho; A. Rosenqvist; Y.E. Shimabukuro; J.R. Santos. Evaluation and perspectives of using multitemporal L-Band SAR data to monitor deforestation in the Brazilian Amazonia. *IEEE Geoscience and Remote Sensing Letters*, vol. 2, n. 4, pp. 409-412, 2005.
- [4] T. Neeff; L.V. Dutra; J.R. Santos; C.C. Freitas; L.S. Araujo. Power spectrum analysis of SAR data for spatial forest characterization in Amazonia. *International Journal of Remote Sensing*, University of Dundee, UK, vol. 26, n. 13, pp. 2851-2864, 2005.
- [5] R. Schröder; J. Puls; I. Hajnsek; F. Jochin; T. Neeff; J. Kono; W.R. Paradella; M.M.Q. Silva; D.M. Valeriano; M.P.F. Costa. MAPSAR: A Small L-Band SAR Mission for Land Observation. *Acta Astronautica*, Oxford, England, vol. 56, n. 2004, pp. 35-43, 2005.
- [6] V.S. Frost; J.A. Stiles; K.S. Shanmugan; J.C. Holtzman. A model for radar images and its application to adaptive digital filtering of multiplicative noise, *IEEE Trans. Pattern Analysis and Machine Intelligence*, vol. 4, n. 2, pp. 157-166, March 1982.
- [7] A. Lopes; R. Touzi; E. Nezri. Adaptive speckle filters and scene heterogeneity. *IEEE Transaction on Geoscience and Remote Sensing*, vol.28, pp.992 -1000, 1990.
- [8] L.V. Dutra; R. Huber. Feature extraction and selection for ERS-1/2 InSAR classification. *International Journal of Remote Sensing*, vol. 20, n.5, pp. 993-1016. 1999.
- [9] P.H. Swain; R.C. King. Two effective feature selection criteria for multispectral remote sensing. LARS technical Note 042673. Purdue University, Indiana. 1973. 6p.
- [10] S.R. Cloude; E. Pottier. A review of target decomposition theorems in radar polarimetry. *IEEE Transactions on Geoscience and Remote Sensing*, vol. 34, n. 2, pp. 498-518, 1996.
- [11] A. Freeman; S.L Durden. A three-component scattering model for polarimetric SAR data. *IEEE Transactions on Geoscience and Remote Sensing*, vol. 36, n.3, pp. 963-973, 1998.